

# A Facile Fabrication of $\text{Fe}_3\text{O}_4/\text{ZnO}$ Core-Shell Submicron Particles With Controlled Size

Kyong-Hoon Choi<sup>1,5</sup>, Weon-Sik Chae<sup>2</sup>, Eun-Mee Kim<sup>2</sup>, Jong-Ho Jun<sup>3</sup>, Jong-Hyung Jung<sup>4</sup>, Yong-Rok Kim<sup>1</sup>, and Jin-Seung Jung<sup>4</sup>

<sup>1</sup>Photon Applied Functional Molecule Research Laboratory, Department of Chemistry, Yonsei University, Seoul 120-749, Korea

<sup>5</sup>Material R&D Division, H & Global Co. Ltd. Soha-Dong, Gwangmyeong-si, Gyeonggi-do 423-050, South Korea

<sup>2</sup>Gangneung Center, Korea Basic Science Institute, Gangneung 210-702, South Korea

<sup>3</sup>Department of Applied Chemistry, Konkuk University, Chungju 380-701, South Korea

<sup>4</sup>Department of chemistry, Gangneung-Wonju national University, Gangneung 210-702, South Korea

Monodispersed superparamagnetic magnetite submicron particles were synthesized by using a one-step solvothermal method. Increasing the volume ratio of ethylene glycol/diethylene glycol (EG/DEG) shows a gradual increase in the size of primary nanograin and secondary  $\text{Fe}_3\text{O}_4$  submicroparticles. To induce the photo-magnetic functionality, we have successfully synthesized the multifunctional core-shell ( $\text{Fe}_3\text{O}_4/\text{ZnO}$ ) submicron particles by atomic layer deposition (ALD) method. Microstructure and magnetic properties of the multifunctional core/shell submicron particles are investigated by field emission scanning electron microscopy (FE-SEM), transmission electron microscopy (TEM), vibrating sample magnetometry (VSM), and photoluminescence spectroscopy.

**Index Terms**—Atomic layer deposition, magnetic submicron particle, photomagnetic core/shell particle, solvothermal method, ZnO.

## I. INTRODUCTION

MAGNETIC nanoparticles in the crystalline, a form of magnetite ( $\text{Fe}_3\text{O}_4$ ), become particularly crucial in research area and are attracting a great deal of attention due to their unique properties including superparamagnetism and low toxicity and their potential applications [1]–[3]. However, these pure nanoparticles are unstable in external environment and tend to aggregate easily, causing difficulties for long-term storage, processing, and applications. To enhance the functionality in existing applications and to explore novel applications, various multifunctional nanoparticles have been fabricated in the direction of increased chemical stability and various functionalities. In this regard, multifunctional nanoparticles possessing core/shell structures have attracted more and more attention for their potential biomedical applications as novel drug-delivery vehicles, enzyme-immobilizing hosts, and diagnostic agents due to their unique characteristics including their magnetic or fluorescent properties [4]–[9].

Up to now, a number of researchers have investigated to fabricate superparamagnetic  $\text{Fe}_3\text{O}_4$  submicron particles with controlled particle size. Among them, Leung and co-workers reported secondary structural  $\text{Fe}_3\text{O}_4$  microparticles which are composed of small primary nanocrystals [10], [11]. This method has led to the synthesis of high-quality  $\text{Fe}_3\text{O}_4$  particles with well-controlled size and shape. Due to their size-dependent magnetic properties, the development of simple method to fabricate magnetic materials with tunable sizes is a significant challenge.

Manuscript received February 21, 2011; revised April 20, 2011, May 02, 2011; accepted May 02, 2011. Date of current version September 23, 2011. Corresponding author: J.-S. Jung (e-mail: jjscm@gwnu.ac.kr).

Color versions of one or more of the figures in this paper are available online at <http://ieeexplore.ieee.org>.

Digital Object Identifier 10.1109/TMAG.2011.2152375

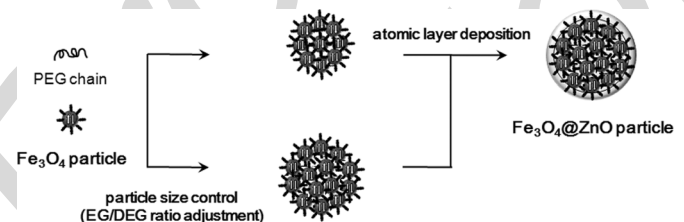


Fig. 1. Fabrication procedure of the multifunctional core-shell submicron particles.

In this study, we have successfully synthesized of multifunctional core/shell ( $\text{Fe}_3\text{O}_4/\text{ZnO}$ ) submicron particles with controlled particle size and shell thickness. In the first step, superparamagnetic  $\text{Fe}_3\text{O}_4$  submicron particles were fabricated by one-step hydrothermal method. The size of core magnetic particle can be tuned rationally by using different amounts of ethylene glycol (EG) and diethylene glycol (DEG). In the second step, the surface of  $\text{Fe}_3\text{O}_4$  submicron particles was coated with ZnO by atomic layer deposition (ALD) method. Through this method, the thickness of shell was accurately tunable.

## II. EXPERIMENT

### A. Preparation of the Multifunctional Particles

The  $\text{Fe}_3\text{O}_4$  submicron particles were prepared by applying a similar method as that in the previous report [12]. Without any other additional chemicals,  $\text{FeCl}_3 \cdot 6\text{H}_2\text{O}$  (0.54 g) and NaAc (1.5 g) were dissolved in EG (20 mL) to form a clear solution, and then this mixture was vigorously stirred for 30 min. As-formed viscous slurry was transferred into a teflon-lined stainless-steel autoclave of 80 mL capacity. The autoclave was heated to and maintained at  $200^\circ\text{C}$  for 10 h, and naturally cooled to room temperature. The obtained black precipitates were collected after being washed with distilled water and absolute alcohol several times and dried at  $60^\circ\text{C}$  for 6 h. The above synthetic method can be extended to synthesize ferrite submicron particles with size

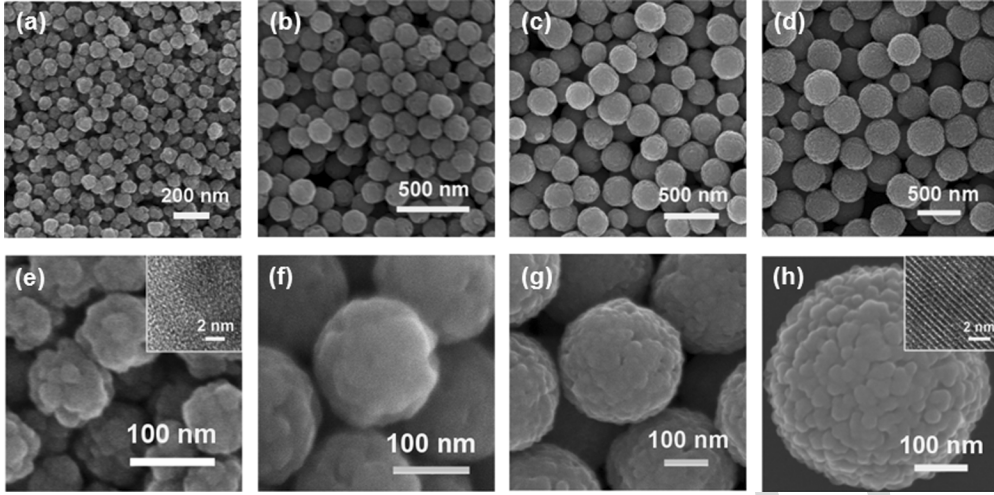


Fig. 2. FE-SEM images of the size-controlled  $\text{Fe}_3\text{O}_4$  submicron particles synthesized by using different ratio of  $V_{\text{EG}}/V_{\text{DEG}}$ : (a) 5/15, 95 nm; (b) 10/10, 175 nm; (c) 15/5, 280 nm; (d) 20/0, 420 nm. The inset represents the high resolution TEM images.

from 90 to 400 nm by varying the  $V_{\text{EG}}/V_{\text{DEG}}$  ratios. The reaction was performed under the same conditions as used for the synthesis of ferrite submicron particles, except that the EG solvent was substituted by EG/DEG mixture solvent (total volume is 20 mL). The ratio of  $V_{\text{EG}}/V_{\text{DEG}}$  controls the size of the  $\text{Fe}_3\text{O}_4$  submicron particles. For example, the ratios of 5/15, 10/10, 15/5 and 20/0 lead to the synthesis of  $\text{Fe}_3\text{O}_4$  submicron particles with average sizes of 95, 175, 280 and 420 nm, respectively.

Functionality on the magnetic particles was provided by ALD process with ZnO as follows. Atomic layers of ZnO were deposited on the  $\text{Fe}_3\text{O}_4$  submicron particles using a Cambridge NanoTech Savannah S100 ALD system, with diethylzinc (DEZn) and  $\text{H}_2\text{O}$  as precursors and a deposition temperature of  $150^\circ\text{C}$ . One cycle of ALD deposition consisted of exposure to DEZn (0.015 s), a 10 s purge, exposure to  $\text{H}_2\text{O}$  (0.05 s) and a 10 s purge.

### B. Characterization of the Multifunctional Particles

To determine the size and surface morphology of the multifunctional submicron particles, field emission scanning electron microscopy (FE-SEM, Hitachi, SU-70) and transmission electron microscopy (TEM, JEOL, JEM-2100F) equipped with an energy dispersive X-ray spectroscopy (EDS) were utilized. The crystallographic characteristics and nanostructure of the composite coatings were investigated with X-ray diffractometer (PANalytical, X'Pert Pro MPD) working on  $\text{Cu K}\alpha$  radiation. A vibrating sample magnetometry (VSM, Lakeshore 7300) was utilized to measure the magnetization versus magnetic field loop at room temperature up to  $H = 10$  kOe. Photoluminescence (PL) and photoluminescence excitation (PLE) spectra were measured on a spectrophotometer (F-7000, Hitachi).

## III. RESULTS AND DISCUSSION

The multifunctional core/shell submicron particles were prepared by a simple surface modification of ALD process with ZnO as shown in Fig. 1. Firstly, the  $\text{Fe}_3\text{O}_4$  submicron particles were prepared by using a solvothermal reduction method.

Through the change of the volume ratio of EG/DEG (v/v in mL), the size of  $\text{Fe}_3\text{O}_4$  particle was controlled in the range of 90–400 nm. And then, the size-controlled particles were coated with ZnO using by ALD process.

Fig. 2 shows the FE-SEM images of the  $\text{Fe}_3\text{O}_4$  submicron particles with the controlled size. All the particles show a spherical morphology with a rough surface. The size of the  $\text{Fe}_3\text{O}_4$  particles can be precisely controlled from 95 nm to 420 nm by simply increasing the ratio of  $V_{\text{EG}}/V_{\text{DEG}}$ . The mean diameter of the prepared  $\text{Fe}_3\text{O}_4$  particles is proportional to the ratio of  $V_{\text{EG}}/V_{\text{DEG}}$  during the solvothermal reaction. When  $V_{\text{EG}}/V_{\text{DEG}}$  was varied from 5/15 to 10/10, 15/5 and 20/0, the diameters of the resulting  $\text{Fe}_3\text{O}_4$  particles were 95, 175, 280 and 420 nm, respectively. As shown in the Fig. 2(e)–(h), the FE-SEM image at high magnification shows that the individual spheres are composed of irregular nanograins with a size of 10–15 nm. To obtain more detailed information of the grain structure of the  $\text{Fe}_3\text{O}_4$  particles, HRTEM image recorded from the edge of an aggregated sphere is shown in the inset of Fig. 2(e), (h). It can be concluded that all assembled small nanograins have regular parallel lattice fringes. The interlayer distance was approximately calculated to be  $\approx 2.97 \text{ \AA}$ , which is comparable to those of the (220) planes in the inverse spinel-structured magnetite nanoparticles [13].

The powder XRD patterns of all controlled  $\text{Fe}_3\text{O}_4$  particles provided more detailed structural information as shown in Fig. 3. The strong Bragg reflection peaks ( $2\theta = 30.0, 35.6, 43.3, 53.7, 57.0, 62.8^\circ$ ), marked by their Miller indices ((220), (311), (400), (422), (511), and (440)) are obtained from standard  $\text{Fe}_3\text{O}_4$  powder diffraction data (JCPDS, card 19-0629). The position and relative intensity of all diffraction peaks match well with the characteristic peaks of magnetite crystal with the cubic inverse spinel structure [14]. To estimate the grain size according to the volume ratio of EG/DEG, the observed diffraction peak profile ( $2\theta = 35.5^\circ$ ) in this study are reasonably well fitted by a convolution of Lorentzian functions (the right side of Fig. 3). The average grain size is calculated based on the Scherrer's equation. With

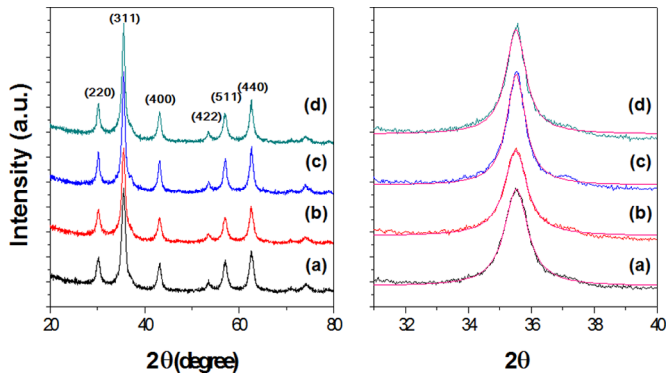


Fig. 3. XRD patterns of the size-controlled  $\text{Fe}_3\text{O}_4$  submicron particles synthesized by using different ratio of  $V_{\text{EG}}/V_{\text{DEG}}$ : (a) 5/15, (b) 10/10, (c) 15/5, and (d) 20/0.

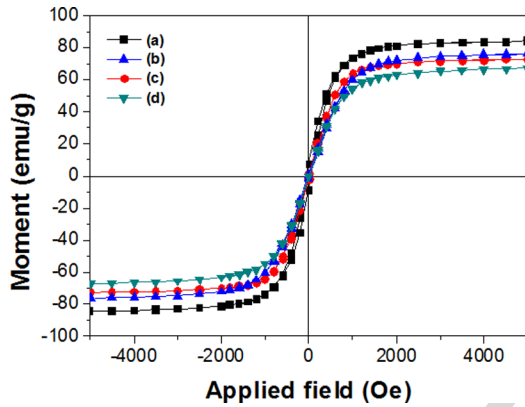


Fig. 4. Room-temperature magnetic hysteresis loops of the size-controlled  $\text{Fe}_3\text{O}_4$  submicron particles which were synthesized by using different ratio of  $V_{\text{EG}}/V_{\text{DEG}}$ : (a) 20/0, (b) 15/5, (c) 10/10, and (d) 5/15.

the increase in the volume ratio of EG, the average sizes of the primary crystallites are increased from 9.2 to 9.7, 11.1, and 15.0 nm, respectively. These results suggest that the grain size of the  $\text{Fe}_3\text{O}_4$  particle shows a gradual increase with increasing the volume ratio of EG. Therefore, the volume ratio of EG/DEG plays an important role forming the particle size and the grain size.

The room-temperature hysteresis loop of the size-controlled  $\text{Fe}_3\text{O}_4$  particles was measured using a vibrating sample magnetometer (VSM). Fig. 4 shows the change in the saturation magnetization for all size-controlled  $\text{Fe}_3\text{O}_4$  particles. The magnetization curves of all samples exhibit no hysteresis, and no coercivity is reached, even at the highest magnetic field. This indicates that all magnetic particles have superparamagnetic behavior. In the present system, the pure  $\text{Fe}_3\text{O}_4$  submicron particle is composed of irregular nanograins with a size of below 15 nm, as observed in the FE-SEM image and X-ray diffraction pattern. Generally, magnetite nanoparticles show superparamagnetic properties when the nanograin size decreases to below 20 nm. This result is well agreed with previous studies that the magnetite submicrospheres composed of small nanograins have superparamagnetic behavior [15], [16]. The observed saturation magnetization ( $M_s$ ) values of  $\text{Fe}_3\text{O}_4$  particles with size of 95, 175, 280, and 420 nm are 67.3, 72.9, 76.3, and 84.3 emu/g, respectively.

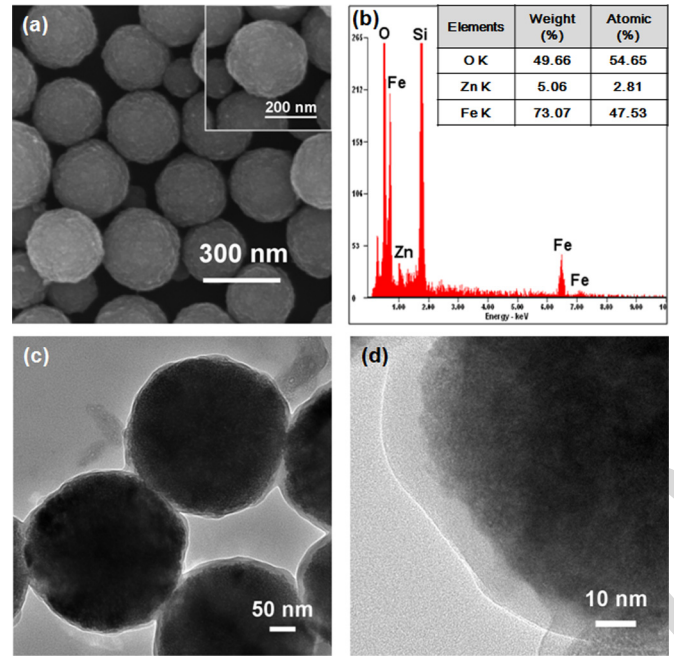


Fig. 5. Morphology and crystal structure of the multifunctional  $\text{Fe}_3\text{O}_4/\text{ZnO}$  particles: (a) FE-SEM micrograph of the multifunctional  $\text{Fe}_3\text{O}_4/\text{ZnO}$  particles; (b) EDX spectrum data of the multifunctional  $\text{Fe}_3\text{O}_4/\text{ZnO}$  particles; (c) and (d) TEM micrographs of the multifunctional  $\text{Fe}_3\text{O}_4/\text{ZnO}$  particles.

By using the ALD process, the size-controlled  $\text{Fe}_3\text{O}_4$  particles can be easily coated with a ZnO layer with a controllable thickness. A total of 100 ALD cycles of ZnO were deposited with DEZn and  $\text{H}_2\text{O}$  used as precursors. Fig. 5(a) shows the FE-SEM image of the multifunctional  $\text{Fe}_3\text{O}_4/\text{ZnO}$  submicron particles. Comparing Fig. 1(g) with Fig. 5(a), one can clearly see that the originally rough surface of  $\text{Fe}_3\text{O}_4$  particles due to small primary nanograins becomes smooth after coating with the thin layer of ZnO. From the FE-SEM image, the mean diameters are estimated to be about 300 nm for the multifunctional  $\text{Fe}_3\text{O}_4/\text{ZnO}$  particles. This result indicates that the diameter of multifunctional  $\text{Fe}_3\text{O}_4/\text{ZnO}$  particles is a little larger than the  $\text{Fe}_3\text{O}_4$  particles. The energy dispersive X-ray analysis (EDXA) of the illuminating electron beams on the obtained  $\text{Fe}_3\text{O}_4/\text{ZnO}$  particles reveals the existence of Fe, Zn, O, and Si elements, further confirming the formation of ZnO species on the  $\text{Fe}_3\text{O}_4$  particles (Fig. 5(b)). The Zn content was 2.81 wt %. The Si peaks were caused by the Si wafer used to support the particles during the analysis. The uniform and nonaggregated nature of the composite particles can be more easily recognized in TEM images (Fig. 5(c), (d)). As it is obvious from the image, the multifunctional  $\text{Fe}_3\text{O}_4/\text{ZnO}$  particles have a mean diameter of  $\sim 300$  nm, confirmed to the FE-SEM observation. Therefore, after the ALD process, the size-controlled  $\text{Fe}_3\text{O}_4$  particles were successfully modified with a thin ZnO layer. At this point, the thickness of the ZnO layer was estimated to be  $\sim 8$  nm.

The ZnO coated iron oxide submicron particles show typical absorption and emission characteristics because of the ZnO coated layer (Fig. 6). The observed PLE spectrum shows the lowest excitation state at 328 nm, which is blue-shifted from the bulk band-gap of 3.37 eV (368 nm) [17], [18]. It may be attributed to quantum confinement effects of ZnO shell

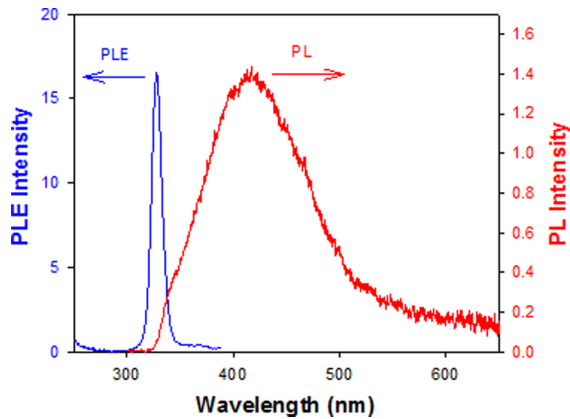


Fig. 6. PL and PLE spectra of the  $\text{Fe}_3\text{O}_4/\text{ZnO}$  core-shell submicron particles. Excitation and detection wavelengths are 280 and 350 nm for the PL and PLE spectra, respectively.

due to the thin layer thickness having a few nanometers. PL spectrum shows a direct band-edge emission at  $\sim 338$  nm as a shoulder and intense emissions centered at  $\sim 420$  nm. Such the red-shifted broad emissions have been typically observed in ZnO nanomaterials, which are assigned to a recombination process through electronic states originating from oxygen vacancies or surface defects [19], [20].

In summary, we are able to control the size of superparamagnetic magnetite submicroparticles from 95 nm to 420 nm by using binary solvent system. The saturation magnetization ( $M_s$ ) of magnetite submicroparticles is determined to be 67.3, 72.9, 76.3, and 84.3 emu/g for 95, 175, 280, and 420 nm particles respectively. The increase in  $\text{Fe}_3\text{O}_4$  particles cause increase in  $M_s$ . Moreover we have successfully synthesized and characterized core-shell ( $\text{Fe}_3\text{O}_4/\text{ZnO}$ ) particles by ALD method.

#### ACKNOWLEDGMENT

This work was supported by the National Research Foundation of Korea Grant funded by the Korean Government (No.

2010-0025875) and the Converging Research Center Program through the National Research Foundation of Korea (NRF) funded by the Ministry of Education, Science and Technology (No. 2010K001115). Prof. Y.-R. Kim thanks a grant from the National Research Foundation of Korea Grant funded by the Korean Government (No. 2010-0025875).

#### REFERENCES

- [1] S. Sun, C. B. Murray, D. Weller, L. Folks, and A. Moser, *Science*, vol. 287, p. 1989, 2000.
- [2] V. Skumryev, S. Stoyanov, Y. Zhang, G. Hadjipanayis, D. Givord, and J. Nogues, *Nature*, vol. 423, p. 850, 2003.
- [3] S. H. Lim, E. J. Woo, H. J. Lee, and C. H. Lee, *Appl. Catal. B*, vol. 85, p. 71, 2008.
- [4] X. Gao, Y. Cui, R. M. Levenson, L. W. K. Chung, and S. Nie, *Nat. Biotechnol.*, vol. 22, p. 969, 2004.
- [5] V. P. Torchilin, *Nat. Rev. Drug Discovery*, vol. 4, p. 145, 2005.
- [6] R. Duncan, *Nat. Rev. Cancer*, vol. 6, p. 688, 2006.
- [7] D. Peer, J. M. Karp, S. Hong, O. C. Farokhzad, R. Margalit, and R. Langer, *Nat. Nanotechnol.*, vol. 2, p. 751, 2007.
- [8] G. D. Liang, J. T. Xu, and X. S. Wang, *J. Am. Chem. Soc.*, vol. 131, p. 5378, 2009.
- [9] Y. Lu, A. Wittemann, and M. Ballauff, *Macromol. Rapid Commun.*, vol. 30, p. 806, 2009.
- [10] S. Xuan, Y. J. Wang, J. C. Yu, and K. C. Leung, *Chem. Mater.*, vol. 21, p. 5079, 2009.
- [11] S. Xuan, F. Wang, Y. J. Wang, J. C. Yu, and K. C. Leung, *J. Mater. Chem.*, vol. 20, p. 5086, 2010.
- [12] H. Deng, X. Li, Q. Peng, X. Wang, J. Chen, and Y. Li, *Angew. Chem. Int. Ed.*, vol. 44, p. 2782, 2005.
- [13] S. Sun, H. Zeng, D. B. Robinson, S. Raoux, P. M. Rice, S. X. Wang, and G. Li, *J. Am. Chem. Soc.*, vol. 126, p. 273, 2003.
- [14] S. F. Chin, K. S. Iyer, and C. L. Raston, *Cryst. Growth. Des.*, vol. 9, p. 2685, 2009.
- [15] J. P. Ge, Y. X. Hu, M. Biasini, W. P. Beyermann, and Y. D. Yin, *Angew. Chem. Int. Ed.*, vol. 46, p. 4342, 2007.
- [16] S. J. Guo, D. Li, L. M. Zhang, J. Li, and E. K. Wang, *Biomaterials*, vol. 30, p. 1881, 2009.
- [17] S. T. Tan, B. J. Chen, X. W. Sun, W. J. Fan, H. S. Kwok, X. H. Zhang, and S. J. Chua, *J. Appl. Phys.*, vol. 98, p. 013505, 2005.
- [18] E. A. Meulenkamp, *J. Phys. Chem. B*, vol. 102, p. 5566, 1998.
- [19] S. Monticone, R. Tufeu, and A. V. Kanaev, *J. Phys. Chem. B*, vol. 102, p. 2854, 1998.
- [20] S.-H. Choi, E.-G. Kim, J. Park, K. An, N. Lee, S. C. Kim, and T. Hyeon, *J. Phys. Chem. B*, vol. 109, p. 14792, 2005.

# A Facile Fabrication of $\text{Fe}_3\text{O}_4/\text{ZnO}$ Core-Shell Submicron Particles With Controlled Size

Kyong-Hoon Choi<sup>1,5</sup>, Weon-Sik Chae<sup>2</sup>, Eun-Mee Kim<sup>2</sup>, Jong-Ho Jun<sup>3</sup>, Jong-Hyung Jung<sup>4</sup>, Yong-Rok Kim<sup>1</sup>, and Jin-Seung Jung<sup>4</sup>

<sup>1</sup>Photon Applied Functional Molecule Research Laboratory, Department of Chemistry, Yonsei University, Seoul 120-749, Korea

<sup>5</sup>Material R&D Division, H & Global Co. Ltd. Soha-Dong, Gwangmyeong-si, Gyeonggi-do 423-050, South Korea

<sup>2</sup>Gangneung Center, Korea Basic Science Institute, Gangneung 210-702, South Korea

<sup>3</sup>Department of Applied Chemistry, Konkuk University, Chungju 380-701, South Korea

<sup>4</sup>Department of chemistry, Gangneung-Wonju national University, Gangneung 210-702, South Korea

Monodispersed superparamagnetic magnetite submicron particles were synthesized by using a one-step solvothermal method. Increasing the volume ratio of ethylene glycol/diethylene glycol (EG/DEG) shows a gradual increase in the size of primary nanograin and secondary  $\text{Fe}_3\text{O}_4$  submicroparticles. To induce the photo-magnetic functionality, we have successfully synthesized the multifunctional core-shell ( $\text{Fe}_3\text{O}_4/\text{ZnO}$ ) submicron particles by atomic layer deposition (ALD) method. Microstructure and magnetic properties of the multifunctional core/shell submicron particles are investigated by field emission scanning electron microscopy (FE-SEM), transmission electron microscopy (TEM), vibrating sample magnetometry (VSM), and photoluminescence spectroscopy.

**Index Terms**—Atomic layer deposition, magnetic submicron particle, photomagnetic core/shell particle, solvothermal method, ZnO.

## I. INTRODUCTION

MAGNETIC nanoparticles in the crystalline, a form of magnetite ( $\text{Fe}_3\text{O}_4$ ), become particularly crucial in research area and are attracting a great deal of attention due to their unique properties including superparamagnetism and low toxicity and their potential applications [1]–[3]. However, these pure nanoparticles are unstable in external environment and tend to aggregate easily, causing difficulties for long-term storage, processing, and applications. To enhance the functionality in existing applications and to explore novel applications, various multifunctional nanoparticles have been fabricated in the direction of increased chemical stability and various functionalities. In this regard, multifunctional nanoparticles possessing core/shell structures have attracted more and more attention for their potential biomedical applications as novel drug-delivery vehicles, enzyme-immobilizing hosts, and diagnostic agents due to their unique characteristics including their magnetic or fluorescent properties [4]–[9].

Up to now, a number of researchers have investigated to fabricate superparamagnetic  $\text{Fe}_3\text{O}_4$  submicron particles with controlled particle size. Among them, Leung and co-workers reported secondary structural  $\text{Fe}_3\text{O}_4$  microparticles which are composed of small primary nanocrystals [10], [11]. This method has led to the synthesis of high-quality  $\text{Fe}_3\text{O}_4$  particles with well-controlled size and shape. Due to their size-dependent magnetic properties, the development of simple method to fabricate magnetic materials with tunable sizes is a significant challenge.

Manuscript received February 21, 2011; revised April 20, 2011, May 02, 2011; accepted May 02, 2011. Date of current version September 23, 2011. Corresponding author: J.-S. Jung (e-mail: jjscm@gwnu.ac.kr).

Color versions of one or more of the figures in this paper are available online at <http://ieeexplore.ieee.org>.

Digital Object Identifier 10.1109/TMAG.2011.2152375

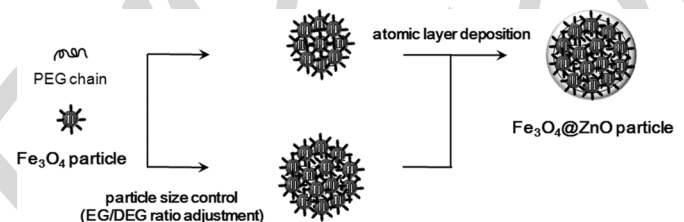


Fig. 1. Fabrication procedure of the multifunctional core-shell submicron particles.

In this study, we have successfully synthesized of multifunctional core/shell ( $\text{Fe}_3\text{O}_4/\text{ZnO}$ ) submicron particles with controlled particle size and shell thickness. In the first step, superparamagnetic  $\text{Fe}_3\text{O}_4$  submicron particles were fabricated by one-step hydrothermal method. The size of core magnetic particle can be tuned rationally by using different amounts of ethylene glycol (EG) and diethylene glycol (DEG). In the second step, the surface of  $\text{Fe}_3\text{O}_4$  submicron particles was coated with ZnO by atomic layer deposition (ALD) method. Through this method, the thickness of shell was accurately tunable.

## II. EXPERIMENT

### A. Preparation of the Multifunctional Particles

The  $\text{Fe}_3\text{O}_4$  submicron particles were prepared by applying a similar method as that in the previous report [12]. Without any other additional chemicals,  $\text{FeCl}_3 \cdot 6\text{H}_2\text{O}$  (0.54 g) and NaAc (1.5 g) were dissolved in EG (20 mL) to form a clear solution, and then this mixture was vigorously stirred for 30 min. As-formed viscous slurry was transferred into a teflon-lined stainless-steel autoclave of 80 mL capacity. The autoclave was heated to and maintained at  $200^\circ\text{C}$  for 10 h, and naturally cooled to room temperature. The obtained black precipitates were collected after being washed with distilled water and absolute alcohol several times and dried at  $60^\circ\text{C}$  for 6 h. The above synthetic method can be extended to synthesize ferrite submicron particles with size

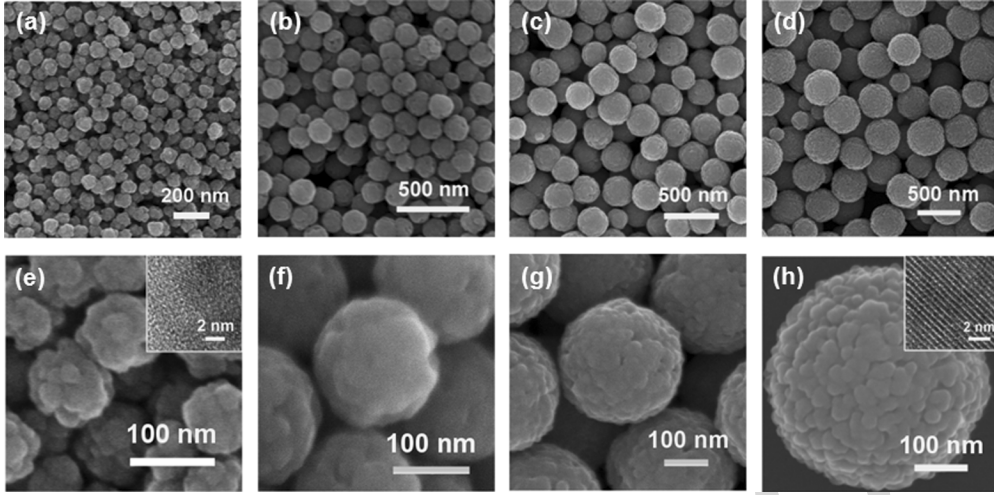


Fig. 2. FE-SEM images of the size-controlled  $\text{Fe}_3\text{O}_4$  submicron particles synthesized by using different ratio of  $V_{\text{EG}}/V_{\text{DEG}}$ : (a) 5/15, 95 nm; (b) 10/10, 175 nm; (c) 15/5, 280 nm; (d) 20/0, 420 nm. The inset represents the high resolution TEM images.

from 90 to 400 nm by varying the  $V_{\text{EG}}/V_{\text{DEG}}$  ratios. The reaction was performed under the same conditions as used for the synthesis of ferrite submicron particles, except that the EG solvent was substituted by EG/DEG mixture solvent (total volume is 20 mL). The ratio of  $V_{\text{EG}}/V_{\text{DEG}}$  controls the size of the  $\text{Fe}_3\text{O}_4$  submicron particles. For example, the ratios of 5/15, 10/10, 15/5 and 20/0 lead to the synthesis of  $\text{Fe}_3\text{O}_4$  submicron particles with average sizes of 95, 175, 280 and 420 nm, respectively.

Functionality on the magnetic particles was provided by ALD process with ZnO as follows. Atomic layers of ZnO were deposited on the  $\text{Fe}_3\text{O}_4$  submicron particles using a Cambridge NanoTech Savannah S100 ALD system, with diethylzinc (DEZn) and  $\text{H}_2\text{O}$  as precursors and a deposition temperature of  $150^\circ\text{C}$ . One cycle of ALD deposition consisted of exposure to DEZn (0.015 s), a 10 s purge, exposure to  $\text{H}_2\text{O}$  (0.05 s) and a 10 s purge.

### B. Characterization of the Multifunctional Particles

To determine the size and surface morphology of the multifunctional submicron particles, field emission scanning electron microscopy (FE-SEM, Hitachi, SU-70) and transmission electron microscopy (TEM, JEOL, JEM-2100F) equipped with an energy dispersive X-ray spectroscopy (EDS) were utilized. The crystallographic characteristics and nanostructure of the composite coatings were investigated with X-ray diffractometer (PANalytical, X'Pert Pro MPD) working on  $\text{Cu K}\alpha$  radiation. A vibrating sample magnetometry (VSM, Lakeshore 7300) was utilized to measure the magnetization versus magnetic field loop at room temperature up to  $H = 10$  kOe. Photoluminescence (PL) and photoluminescence excitation (PLE) spectra were measured on a spectrophotometer (F-7000, Hitachi).

## III. RESULTS AND DISCUSSION

The multifunctional core/shell submicron particles were prepared by a simple surface modification of ALD process with ZnO as shown in Fig. 1. Firstly, the  $\text{Fe}_3\text{O}_4$  submicron particles were prepared by using a solvothermal reduction method.

Through the change of the volume ratio of EG/DEG (v/v in mL), the size of  $\text{Fe}_3\text{O}_4$  particle was controlled in the range of 90–400 nm. And then, the size-controlled particles were coated with ZnO using by ALD process.

Fig. 2 shows the FE-SEM images of the  $\text{Fe}_3\text{O}_4$  submicron particles with the controlled size. All the particles show a spherical morphology with a rough surface. The size of the  $\text{Fe}_3\text{O}_4$  particles can be precisely controlled from 95 nm to 420 nm by simply increasing the ratio of  $V_{\text{EG}}/V_{\text{DEG}}$ . The mean diameter of the prepared  $\text{Fe}_3\text{O}_4$  particles is proportional to the ratio of  $V_{\text{EG}}/V_{\text{DEG}}$  during the solvothermal reaction. When  $V_{\text{EG}}/V_{\text{DEG}}$  was varied from 5/15 to 10/10, 15/5 and 20/0, the diameters of the resulting  $\text{Fe}_3\text{O}_4$  particles were 95, 175, 280 and 420 nm, respectively. As shown in the Fig. 2(e)–(h), the FE-SEM image at high magnification shows that the individual spheres are composed of irregular nanograins with a size of 10–15 nm. To obtain more detailed information of the grain structure of the  $\text{Fe}_3\text{O}_4$  particles, HRTEM image recorded from the edge of an aggregated sphere is shown in the inset of Fig. 2(e), (h). It can be concluded that all assembled small nanograins have regular parallel lattice fringes. The interlayer distance was approximately calculated to be  $\approx 2.97$  Å, which is comparable to those of the (220) planes in the inverse spinel-structured magnetite nanoparticles [13].

The powder XRD patterns of all controlled  $\text{Fe}_3\text{O}_4$  particles provided more detailed structural information as shown in Fig. 3. The strong Bragg reflection peaks ( $2\theta = 30.0, 35.6, 43.3, 53.7, 57.0, 62.8^\circ$ ), marked by their Miller indices ((220), (311), (400), (422), (511), and (440)) are obtained from standard  $\text{Fe}_3\text{O}_4$  powder diffraction data (JCPDS, card 19-0629). The position and relative intensity of all diffraction peaks match well with the characteristic peaks of magnetite crystal with the cubic inverse spinel structure [14]. To estimate the grain size according to the volume ratio of EG/DEG, the observed diffraction peak profile ( $2\theta = 35.5^\circ$ ) in this study are reasonably well fitted by a convolution of Lorentzian functions (the right side of Fig. 3). The average grain size is calculated based on the Scherrer's equation. With

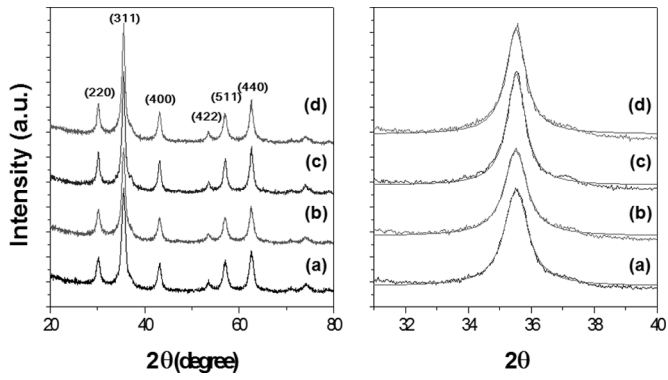


Fig. 3. XRD patterns of the size-controlled  $\text{Fe}_3\text{O}_4$  submicron particles synthesized by using different ratio of  $V_{\text{EG}}/V_{\text{DEG}}$ : (a) 5/15, (b) 10/10, (c) 15/5, and (d) 20/0.

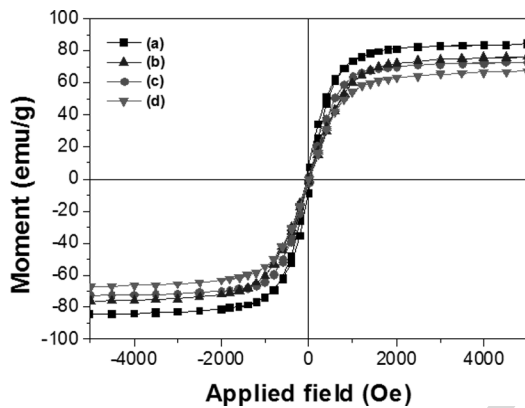


Fig. 4. Room-temperature magnetic hysteresis loops of the size-controlled  $\text{Fe}_3\text{O}_4$  submicron particles which were synthesized by using different ratio of  $V_{\text{EG}}/V_{\text{DEG}}$ : (a) 20/0, (b) 15/5, (c) 10/10, and (d) 5/15.

the increase in the volume ratio of EG, the average sizes of the primary crystallites are increased from 9.2 to 9.7, 11.1, and 15.0 nm, respectively. These results suggest that the grain size of the  $\text{Fe}_3\text{O}_4$  particle shows a gradual increase with increasing the volume ratio of EG. Therefore, the volume ratio of EG/DEG plays an important role forming the particle size and the grain size.

The room-temperature hysteresis loop of the size-controlled  $\text{Fe}_3\text{O}_4$  particles was measured using a vibrating sample magnetometer (VSM). Fig. 4 shows the change in the saturation magnetization for all size-controlled  $\text{Fe}_3\text{O}_4$  particles. The magnetization curves of all samples exhibit no hysteresis, and no coercivity is reached, even at the highest magnetic field. This indicates that all magnetic particles have superparamagnetic behavior. In the present system, the pure  $\text{Fe}_3\text{O}_4$  submicron particle is composed of irregular nanograins with a size of below 15 nm, as observed in the FE-SEM image and X-ray diffraction pattern. Generally, magnetite nanoparticles show superparamagnetic properties when the nanograin size decreases to below 20 nm. This result is well agreed with previous studies that the magnetite submicrospheres composed of small nanograins have superparamagnetic behavior [15], [16]. The observed saturation magnetization ( $M_s$ ) values of  $\text{Fe}_3\text{O}_4$  particles with size of 95, 175, 280, and 420 nm are 67.3, 72.9, 76.3, and 84.3 emu/g, respectively.

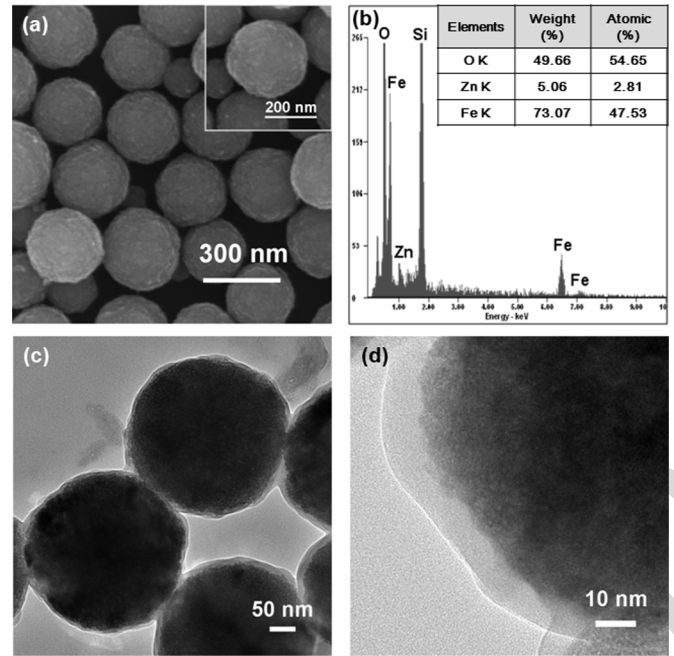


Fig. 5. Morphology and crystal structure of the multifunctional  $\text{Fe}_3\text{O}_4/\text{ZnO}$  particles: (a) FE-SEM micrograph of the multifunctional  $\text{Fe}_3\text{O}_4/\text{ZnO}$  particles; (b) EDX spectrum data of the multifunctional  $\text{Fe}_3\text{O}_4/\text{ZnO}$  particles; (c) and (d) TEM micrographs of the multifunctional  $\text{Fe}_3\text{O}_4/\text{ZnO}$  particles.

By using the ALD process, the size-controlled  $\text{Fe}_3\text{O}_4$  particles can be easily coated with a ZnO layer with a controllable thickness. A total of 100 ALD cycles of ZnO were deposited with DEZn and  $\text{H}_2\text{O}$  used as precursors. Fig. 5(a) shows the FE-SEM image of the multifunctional  $\text{Fe}_3\text{O}_4/\text{ZnO}$  submicron particles. Comparing Fig. 1(g) with Fig. 5(a), one can clearly see that the originally rough surface of  $\text{Fe}_3\text{O}_4$  particles due to small primary nanograins becomes smooth after coating with the thin layer of ZnO. From the FE-SEM image, the mean diameters are estimated to be about 300 nm for the multifunctional  $\text{Fe}_3\text{O}_4/\text{ZnO}$  particles. This result indicates that the diameter of multifunctional  $\text{Fe}_3\text{O}_4/\text{ZnO}$  particles is a little larger than the  $\text{Fe}_3\text{O}_4$  particles. The energy dispersive X-ray analysis (EDXA) of the illuminating electron beams on the obtained  $\text{Fe}_3\text{O}_4/\text{ZnO}$  particles reveals the existence of Fe, Zn, O, and Si elements, further confirming the formation of ZnO species on the  $\text{Fe}_3\text{O}_4$  particles (Fig. 5(b)). The Zn content was 2.81 wt %. The Si peaks were caused by the Si wafer used to support the particles during the analysis. The uniform and nonaggregated nature of the composite particles can be more easily recognized in TEM images (Fig. 5(c), (d)). As it is obvious from the image, the multifunctional  $\text{Fe}_3\text{O}_4/\text{ZnO}$  particles have a mean diameter of  $\sim 300$  nm, confirmed to the FE-SEM observation. Therefore, after the ALD process, the size-controlled  $\text{Fe}_3\text{O}_4$  particles were successfully modified with a thin ZnO layer. At this point, the thickness of the ZnO layer was estimated to be  $\sim 8$  nm.

The ZnO coated iron oxide submicron particles show typical absorption and emission characteristics because of the ZnO coated layer (Fig. 6). The observed PLE spectrum shows the lowest excitation state at 328 nm, which is blue-shifted from the bulk band-gap of 3.37 eV (368 nm) [17], [18]. It may be attributed to quantum confinement effects of ZnO shell

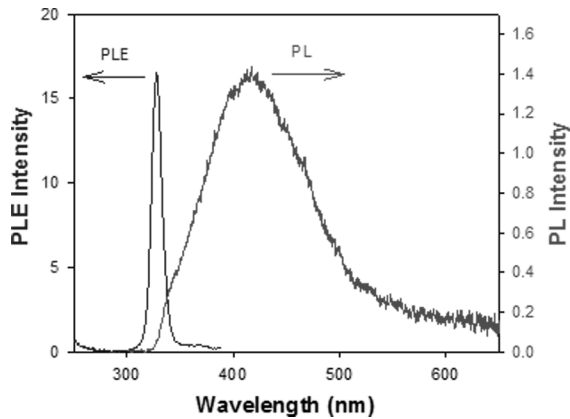


Fig. 6. PL and PLE spectra of the  $\text{Fe}_3\text{O}_4/\text{ZnO}$  core-shell submicron particles. Excitation and detection wavelengths are 280 and 350 nm for the PL and PLE spectra, respectively.

due to the thin layer thickness having a few nanometers. PL spectrum shows a direct band-edge emission at  $\sim 338$  nm as a shoulder and intense emissions centered at  $\sim 420$  nm. Such the red-shifted broad emissions have been typically observed in ZnO nanomaterials, which are assigned to a recombination process through electronic states originating from oxygen vacancies or surface defects [19], [20].

In summary, we are able to control the size of superparamagnetic magnetite submicroparticles from 95 nm to 420 nm by using binary solvent system. The saturation magnetization ( $M_s$ ) of magnetite submicroparticles is determined to be 67.3, 72.9, 76.3, and 84.3 emu/g for 95, 175, 280, and 420 nm particles respectively. The increase in  $\text{Fe}_3\text{O}_4$  particles cause increase in  $M_s$ . Moreover we have successfully synthesized and characterized core-shell ( $\text{Fe}_3\text{O}_4/\text{ZnO}$ ) particles by ALD method.

#### ACKNOWLEDGMENT

This work was supported by the National Research Foundation of Korea Grant funded by the Korean Government (No.

2010-0025875) and the Converging Research Center Program through the National Research Foundation of Korea (NRF) funded by the Ministry of Education, Science and Technology (No. 2010K001115). Prof. Y.-R. Kim thanks a grant from the National Research Foundation of Korea Grant funded by the Korean Government (No. 2010-0025875).

#### REFERENCES

- [1] S. Sun, C. B. Murray, D. Weller, L. Folks, and A. Moser, *Science*, vol. 287, p. 1989, 2000.
- [2] V. Skumryev, S. Stoyanov, Y. Zhang, G. Hadjipanayis, D. Givord, and J. Nogues, *Nature*, vol. 423, p. 850, 2003.
- [3] S. H. Lim, E. J. Woo, H. J. Lee, and C. H. Lee, *Appl. Catal. B*, vol. 85, p. 71, 2008.
- [4] X. Gao, Y. Cui, R. M. Levenson, L. W. K. Chung, and S. Nie, *Nat. Biotechnol.*, vol. 22, p. 969, 2004.
- [5] V. P. Torchilin, *Nat. Rev. Drug Discovery*, vol. 4, p. 145, 2005.
- [6] R. Duncan, *Nat. Rev. Cancer*, vol. 6, p. 688, 2006.
- [7] D. Peer, J. M. Karp, S. Hong, O. C. Farokhzad, R. Margalit, and R. Langer, *Nat. Nanotechnol.*, vol. 2, p. 751, 2007.
- [8] G. D. Liang, J. T. Xu, and X. S. Wang, *J. Am. Chem. Soc.*, vol. 131, p. 5378, 2009.
- [9] Y. Lu, A. Wittemann, and M. Ballauff, *Macromol. Rapid Commun.*, vol. 30, p. 806, 2009.
- [10] S. Xuan, Y. J. Wang, J. C. Yu, and K. C. Leung, *Chem. Mater.*, vol. 21, p. 5079, 2009.
- [11] S. Xuan, F. Wang, Y. J. Wang, J. C. Yu, and K. C. Leung, *J. Mater. Chem.*, vol. 20, p. 5086, 2010.
- [12] H. Deng, X. Li, Q. Peng, X. Wang, J. Chen, and Y. Li, *Angew. Chem. Int. Ed.*, vol. 44, p. 2782, 2005.
- [13] S. Sun, H. Zeng, D. B. Robinson, S. Raoux, P. M. Rice, S. X. Wang, and G. Li, *J. Am. Chem. Soc.*, vol. 126, p. 273, 2003.
- [14] S. F. Chin, K. S. Iyer, and C. L. Raston, *Cryst. Growth. Des.*, vol. 9, p. 2685, 2009.
- [15] J. P. Ge, Y. X. Hu, M. Biasini, W. P. Beyermann, and Y. D. Yin, *Angew. Chem. Int. Ed.*, vol. 46, p. 4342, 2007.
- [16] S. J. Guo, D. Li, L. M. Zhang, J. Li, and E. K. Wang, *Biomaterials*, vol. 30, p. 1881, 2009.
- [17] S. T. Tan, B. J. Chen, X. W. Sun, W. J. Fan, H. S. Kwok, X. H. Zhang, and S. J. Chua, *J. Appl. Phys.*, vol. 98, p. 013505, 2005.
- [18] E. A. Meulenkamp, *J. Phys. Chem. B*, vol. 102, p. 5566, 1998.
- [19] S. Monticone, R. Tufeu, and A. V. Kanaev, *J. Phys. Chem. B*, vol. 102, p. 2854, 1998.
- [20] S.-H. Choi, E.-G. Kim, J. Park, K. An, N. Lee, S. C. Kim, and T. Hyeon, *J. Phys. Chem. B*, vol. 109, p. 14792, 2005.